Progress In Electromagnetics Research, Vol. 140, 781–794, 2013

MILLIMETER WAVE SUBHARMONIC MIXER IMPLEMENTATION USING GRAPHENE FILM COATING

George Hotopan*, Samuel Ver Hoeye, Carlos Vazquez, Andreea Hadarig, Rene Camblor, Miguel Fernández, and Fernando Las Heras

Area of Signal Theory and Communications, Department of Electrical Engineering, University of Oviedo, Campus de Viesques, Edificio Polivalente s/n, mod. 8, 1a planta E-33203, Gijón, Spain

Abstract—In this work, a subharmonic frequency mixer for millimeter wave applications has been designed. The mixing and multiplication phenomena are simultaneously achieved via a nonlinear component consisting in a microstrip line gap covered by a graphene film coating. The circuit structure is made up of various filters, which have been optimized to ensure high port-to-port isolation. The nonlinear behavior of the subharmonic frequency mixer has been experimentally evaluated within the 39–40.5 GHz RF frequency band. The frequency downconversion is achieved by mixing the RF signal with the second harmonic component of a 17.9 GHz LO signal. Conversion losses are minimized by generating a return path for IF, through the use of a quarter wavelength open-ended stub.

1. INTRODUCTION

During the last years, RF system designers and service providers have been confronted with the issue of microwave's spectrum everly increasing congestion. However, due to the rapid development in technology, especially from a manufacturing point of view, a moderate but constant transition to higher frequency bands is taking place. With the fabrication constraints almost gone, circuits at millimeter and submillimeter frequencies are becoming the main topic for many scientists. Factors such as size reduction, higher data rate transmissions, increased security of communications or high spatial resolution play a decisive role in applications oriented toward imaging, medicine, satellite communications, security and defense [1–10].

Received 24 April 2013, Accepted 22 June 2013, Scheduled 3 July 2013

* Corresponding author: George Hotopan (ghotopan@tsc.uniovi.es).

Modern millimeter wave communication systems have strict requirements in terms of cost and performance. One of the fundamental blocks in many systems is the frequency mixer module. For fundamental mixers, the frequency conversion is realized by mixing the RF input signal with the first harmonic of the LO signal, i.e., $f_{IF} = |f_{RF} - f_{LO}|$ (downconversion). Usually, in this type of circuits the frequency difference between the input signals is quite small. At millimeter wave frequencies, it may sometimes be difficult to meet the power requirements with such signal distribution. Subharmonic mixers offer an alternative to fundamental mixers in that the LO frequency is at some integer fraction $1/n$ of the fundamental LO frequency $f_{IF} = |f_{RF} - (n \times f_{LO})|$. The main benefit of this approach is that it allows the use of an LO at a relatively low frequency, where the output power and phase noise performance may be superior to those available at the fundamental frequency. Another advantage is that the wide frequency gap between the RF and LO signals simplifies the LO and RF separation. Frequency mixer circuits, either in microstrip [11–13] or in monolithic technology [14–18], generally use transistors [19–24], or diodes [25–28], in order to generate the desired nonlinear behavior.

The current work is focused on designing a microstrip millimeter wave subharmonic mixer, which uses graphene as nonlinear component. The very large carrier mobility for both electrons and holes in graphene ($\cong$ 200.000 $\mathrm{cm^2V^{-1}s^{-1}}$ around 300 K if extrinsic disorder is eliminated), being at least one order of magnitude higher than in Si and GaAs [29], makes it an interesting choice for high frequency applications. In [30, 31], theoretical analyses on the nonlinear electromagnetic behavior of graphene revealed frequency multiplication/mixing phenomena up into the terahertz frequency spectrum. In [32], authors have demonstrated the nonlinear capabilities of this material by designing a fundamental frequency mixer. In this work, graphene is used not only for the mixing operation between the two input signals, but also to internally multiply the fundamental LO signal, with both operations within the same stage.

The proposed microstrip subharmonic mixer is used to downconvert a millimeter wave Ka band RF input signal ($f_{RF} = 39.75$ GHz) to an intermediate frequency ($f_{IF} = 3.95$ GHz), by mixing the input signal with the second harmonic component of a fundamental LO signal ($f_{LO} = 17.9$ GHz). The proposed topology for the graphene based microstrip subharmonic mixer is described in Section 2.1. In Section 2.2, the design, optimization and simulated results of the circuit input/output blocks are explained. A quarter wavelength open-ended stub is then placed before the multiplying/mixing stage in order to provide a virtual ground and create a return path for IF. The measured

results of the manufactured input/output blocks are presented in Section 3. In Section 4, the nonlinear behavior of graphene is illustrated through a series of power sweeps of the two input signals. The effect of the quarter wavelength open-ended stub on circuit performance is also demonstrated.

2. TOPOLOGY AND DESIGN OF THE MILLIMETER WAVE SUBHARMONIC MIXER

2.1. Topology

The topology of the circuit is presented in Fig. 1. The circuit is designed to behave as a frequency downconverter from Ka band, with $f_{RF} = 39.75\,\text{GHz}$, to an intermediate frequency $f_{IF} = 3.95\,\text{GHz}$, by using the second harmonic component of a fundamental LO signal with $f_{LO} = 17.9\,\text{GHz}$. The frequency selection of the two input signals is achieved by means of two bandpass filters, while the resulting intermodulation product at $f_{IF} = |f_{RF} - (2 \times f_{LO})|$ is extracted at the output port, through a lowpass filtering structure. The nonlinear component consists of a thin film coating of few layer graphene, exfoliated from a highly oriented pyrolithic graphite, and placed along a small microstrip gap. In order to ensure a virtual ground at the multiplying/mixing stage, a quarter wavelength open-ended stub at f_{IF} is placed. In doing so, we ensure a return path for the IF current, optimizing the circuit performance in terms of conversion losses.

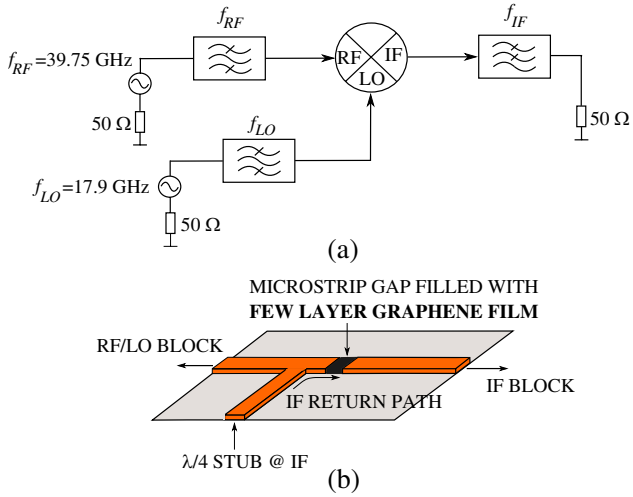

Figure 1. Topology of the subharmonic mixer. (a) Topology. (b) Mixing/multiplying stage.

2.2. Circuit Design

The filters have been designed using both schematic and electromagnetic simulators (Method of Moments — MoM) of Agilent ADS. The dielectric substrate chosen was 0.236 mm thick ARLON 25N ($\epsilon_r = 3.38$, $\tan\delta = 0.0025$ at 10 GHz). The input signals are delivered to the circuit using SouthWest Microwave 2.4 mm SMI end launch connectors. The same type of connector was used at the output to extract the IF signal. The five-pole millimeter wave bandpass filters have been implemented using parallel-coupled, half wavelength resonator microstrip lines (positioned so that adjacent resonators are parallel to each other along half of their length). The filters have been optimized to provide minimum insertion losses and high isolation between the input ports throughout the frequency bands of interest. The interconnection between the two input branches of the subharmonic mixer was realized using a microstrip diplexer, designed and optimized first in the schematic simulator. During the optimization process, a small degree of freedom was given to the dimensions of the bandpass filters. For the implementation of the lowpass output filter, an Arbitrarily Width Modulated Microstrip Line (AWMML) was employed [33]. The AWMML based filter is basically a structure composed of a large number of tapered microstrip sections of identical length. To ensure a smooth transition between adjacent sections, the width modulating function is chosen to be continuous, in a way that the end width of a microstrip taper is equal to the begin width of the next one. Further details regarding the design and optimization of this kind of structure have been presented in [32].

For simulation purposes, the whole circuit was divided into two blocks: the first block contains the two microstrip bandpass filters with the diplexer up to the microstrip gap, while the AWMML lowpass filter forms the second block. To create a return path for the IF current, a quarter wavelength open-ended stub at f_{IF} was placed in shunt with the microstrip line at the end of the input block. The distance between the stub and the microstrip gap was chosen such that it looks sufficiently small at f_{IF}. The quarter wavelength open-ended stub guarantees that at $\lambda/4$ away (interconnection point between the stub and the 50 Ω microstrip line) the IF side sees a short circuit. The position of the stub with respect to the microstrip gap does not affect the frequency performance of the bandpass filters. In other words, the stub does not behave as a matching network for the input block. Nevertheless, as it will be shown in Section 4, the placement of the stub affects considerably the performance of the circuit in terms of output power.

From the electromagnetic MoM simulations in Figs. 2 and 3 it can

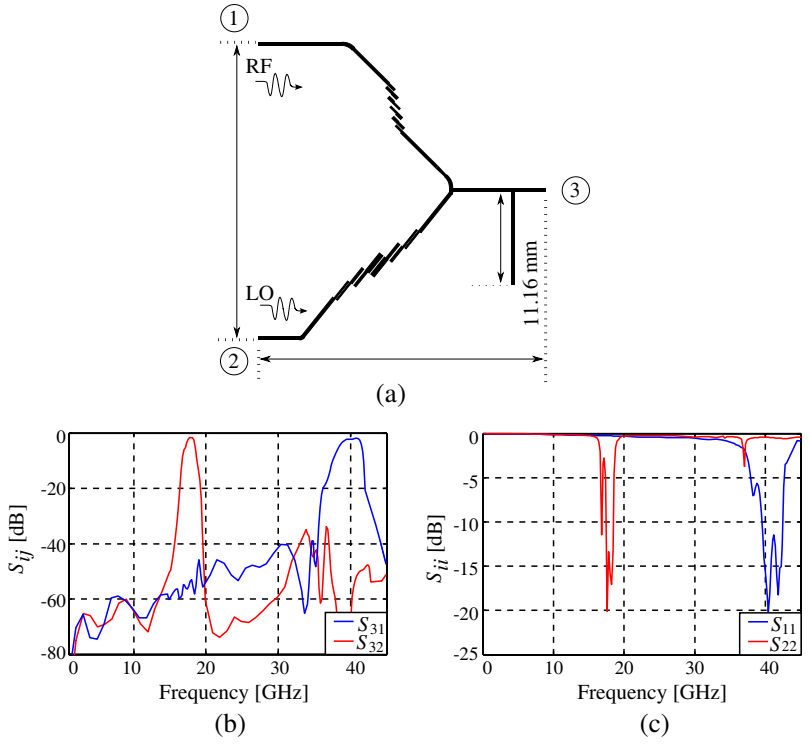

Figure 2. Layout and electromagnetic simulations of input block. (a) Input block. (b) Transmission coefficient. (c) Reflection coefficient.

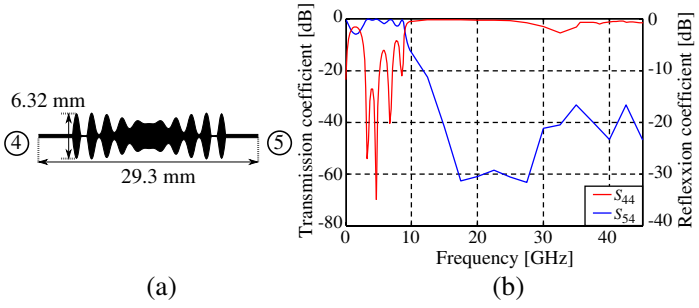

Figure 3. Layout and electromagnetic simulations of AWMML filter. (a) Output block (AWMML filter). (b) S parameters.

be seen that all filters provide low insertion loss values ($S_{31} = -2\,\text{dB}$, $S_{32} = -2\,\text{dB}$ and $S_{54} = -0.5\,\text{dB}$) and high isolation between the input ports. The fractional bandwidth of the filters is $FBW_{RF} \cong 5.5\%$, $FBW_{LO} \cong 7\%$ respectively $FBW_{IF} \cong 110\%$.

In order to assess the effect of the stub placement toward the frequency behavior of the two input filters, a series of electromagnetic simulations were realized for various stub positions. It can be seen from Fig. 4 that moving the quarter wavelength open-ended stub along the 50 Ω microstrip line has a very limited effect on the frequency response of the two bandpass filters.

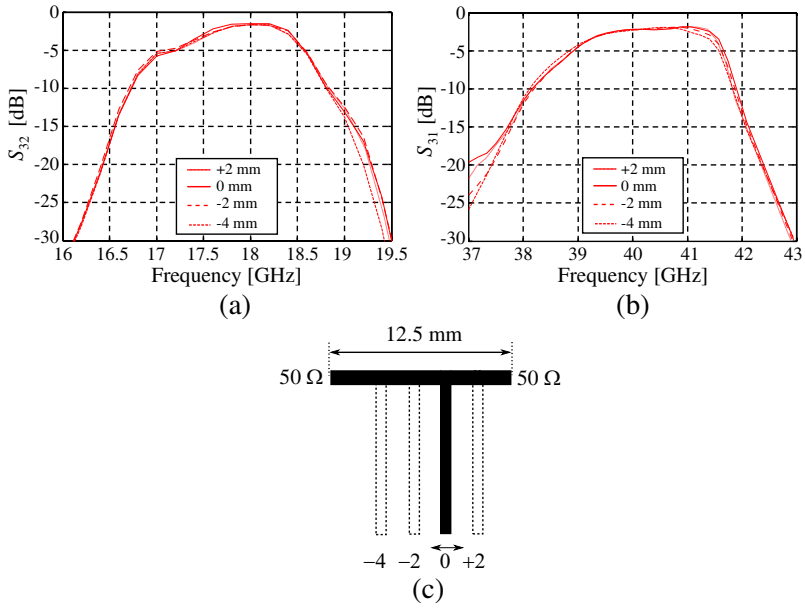

Figure 4. Frequency behavior for various stub positions along the microstrip line. (a) Transmission coefficient f_{LO}. (b) Transmission coefficient f_{RF}. (c) Stub displacement.

3. MEASURED RESULTS

For the validation of the filter designs, two prototypes have been manufactured using laser micromachining. As previously described, the whole circuit was divided in two, with the first prototype containing all elements of the mixer from the input ports 1, 2 to the microstrip line on the left side of the gap (port 3), and a second prototype containing the elements from the right side of the gap (port 4) to the output port 5.

The measured results illustrated in Fig. 5 are in good agreement with the MoM electromagnetic simulations presented in Figs. 2 and 3. Both bandpass filters present low insertion loss values ($S_{31} \cong -2.2$ dB and $S_{32} \cong -2.2$ dB at their corresponding central frequencies) and high

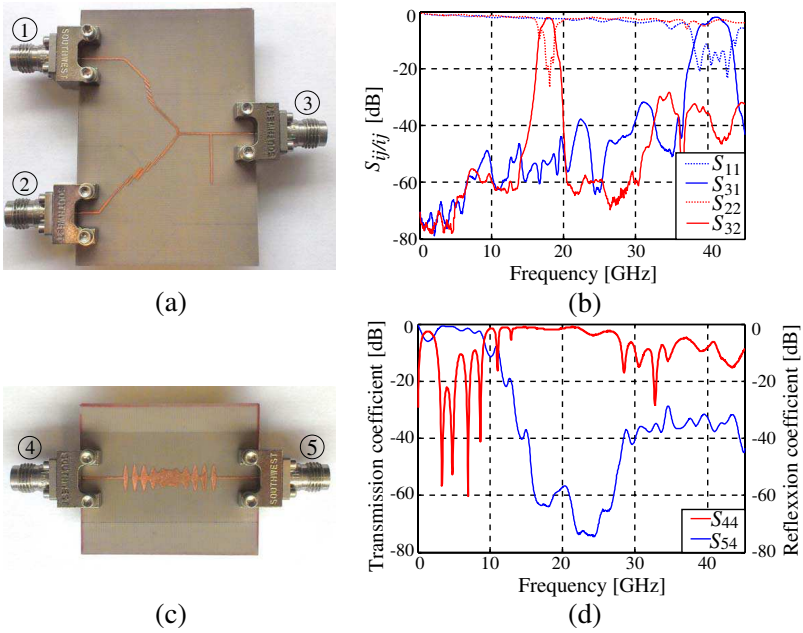

Figure 5. Measured results — input/output block prototypes. (a) Prototype — input block. (b) S parameters. (c) Prototype — output block (AWMML filter). (d) S parameters.

isolation between the input ports ($\geq 30\,\text{dB}$). The measured fractional bandwidth of both filters is very similar to the simulated results, being $FBW_{RF} \cong 5\%$, respectively $FBW_{LO} \cong 6\%$. The AWMML prototype presents insertion loss values as low as $S_{54} \cong -0.8\,\text{dB}$, and a fractional bandwidth $FBW_{IF} \cong 85\%$, slightly smaller than in simulations.

4. EXPERIMENTAL VALIDATION OF THE GRAPHENE BASED SUBHARMONIC MIXER

In order to evaluate the performance of the microstrip millimeter wave subharmonic mixer, a prototype of the complete circuit was manufactured. A small gap was micromachined accross the $50\,\Omega$ microstrip line that connects the diplexer with the IF side. The microstrip gap is covered by a thin film coating of few layer graphene, exfoliated from a highly oriented pyrolithic graphite.

A photo of the graphene based subharmonic mixer prototype is presented in Fig. 6(a). High LO, RF and IF port-to-port isolation was measured within the frequency bands of interest, with overall values better than 45 dB (RF/IF $\geq 45\,\text{dB}$, LO/IF $\geq 60\,\text{dB}$ and RF/LO

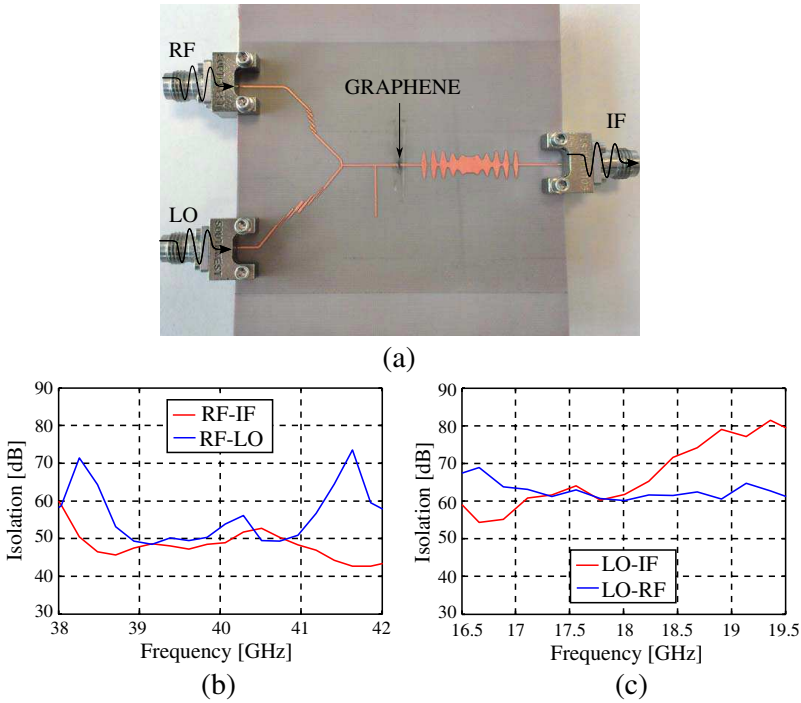

Figure 6. Measured port-to port isolation. (a) Subharmonic mixer prototype. (b) Port-to-port isolation. (c) Port-to-port isolation.

≥ 48 dB), as depicted in Figs. 6(b), (c).

For the experimental validation of the graphene based subharmonic mixer, the RF frequency signal was swept from 39 GHz to 40.5 GHz, for a constant 17.9 GHz LO signal (for the frequency down-conversion, the second harmonic component of the LO signal was used). The IF output signal power was measured within the 3.2 GHz–4.7 GHz frequency band, for different power values of the RF input signal $-9\,\text{dBm} \leq P_{RF} \leq 9\,\text{dBm}$ and LO signal $-3\,\text{dBm} \leq P_{LO} \leq 17\,\text{dBm}$.

From Figs. 7(a), (b) it can be seen that for every 1 dB increase in P_{RF}, P_{OUT} increases by 1 dB, whereas for every 1 dB increase in P_{LO}, P_{OUT} increases by 2 dB. Note that, the measured output power P_{OUT} is not yet limited by any saturation effects, if not by the available local oscillator power P_{LO}. In addition, the efficiency of the mixing/multiplying stage of the graphene based subharmonic mixer is almost frequency independent. The fact that it is not entirely flat is mainly due to the frequency response of the filters involved. Fig. 7(c) presents the output power signal spectrum, where the IF, LO and RF tones can be clearly distinguished.

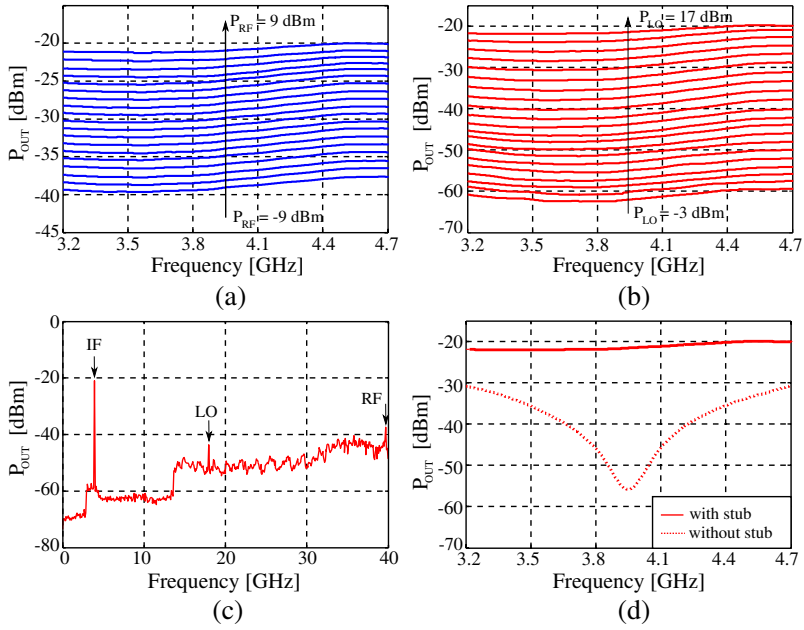

Figure 7. Measured P_{OUT} in terms of P_{RF} and P_{LO}. (a) Measured P_{OUT} when varying P_{RF}. (b) Measured P_{OUT} when varying P_{LO}. (c) Measured P_{OUT} spectrum. (d) Measured P_{OUT} w/o stub.

In order to evaluate the influence of the quarter wavelength open-ended stub on circuit frequency conversion efficiency, the subharmonic mixer prototype was modified by carefully removing the microstrip stub. As shown in Fig. 7(d), the absence of the stub drastically diminishes circuit performance. This is because the circuit is not being provided with an IF return path for the current that biases the graphene based nonlinear component. Placing the quarter wavelength open-ended stub a $\lambda/4$ distance away from the graphene based nonlinear component would have produced a similar frequency response as of "without stub", due to the zero current state condition at IF (the IF side sees an open circuit when looking into the RF/LO block). Measurements of the output power for a single frequency point ($f_{RF} = 39.75\,\text{GHz}$) were also taken, by simultaneously varying the power levels of both injected signals Fig. 8.

An overview of the subharmonic mixer performance is presented in Table 1, comparing it with recently published scientific works, where: GFC — graphene film coating; G-FET — graphene field effect transistor; Type — fundamental (F) or subharmonic (S) mixer; LO-RF — isolation between input ports; CL — conversion loss.

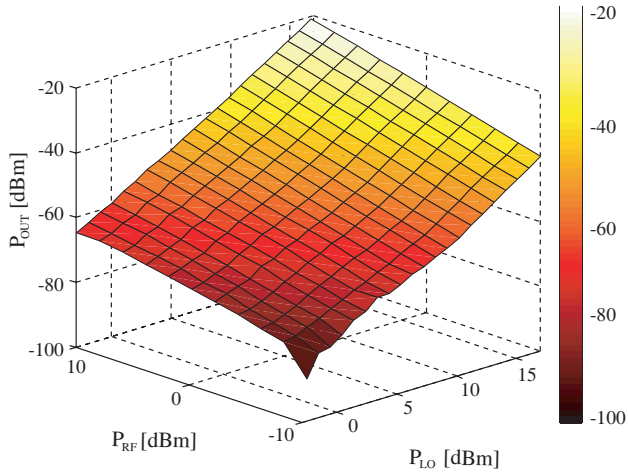

Figure 8. Measured P_{OUT} when varying both P_{RF} and P_{LO} (3.95 GHz).

Table 1. Subharmonic mixer overview and comparison with other works.

	[32]	[34]	[35]	[36]	Current work
Technology	GFC	G-FET	G-FET	G-FET	GFC
Type	F	S	S	F	S
f_{RF} [GHz]	39.3	30.1	3.5	3.8	39.75
LO-RF [dB]	≥ 41	≥ 20	≥ 40	n.a.	≥ 48
CL [dB]	40	20	20–22	27	29

5. CONCLUSIONS

A microstrip millimeter wave subharmonic mixer operating within the 39 GHz–41.5 GHz RF frequency band has been presented. The frequency downconversion is achieved through the implementation of a nonlinear element consisting in a microstrip gap covered by a graphene film coating, exfoliated from a highly oriented pyrolytic graphite. In the mixing process, the second harmonic component of a fundamental LO signal (f_{LO} = 17.9 GHz) was used. The power measurements show a very flat frequency response of the subharmonic mixer over the whole RF frequency band. Conversion losses (CL = 29 dB) were minimized through the proper use of a quarter wavelength open-ended stub, placed in the vicinity of the graphene based nonlinear component.

ACKNOWLEDGMENT

This work has been supported by the "Ministerio de Ciencia e Innovación of Spain /FEDER" under projects IPT-2011-0951-390000 (TECNIGRAF), TEC2011-24491 (ISCAT), CONSOLIDER-INGENIO CSD2008-00068 (TERASENSENSE) and grant AP2012-2020, by the "Gobierno del Principado de Asturias (PCTI)/FEDER-FSE" under projects EQUIP08-06, FC09-COF09-12, EQUIP10-31 and PC10-06 and by "Cátedra Telefónica - Universidad de Oviedo".

REFERENCES

1. Hung, C. Y., M. H. Weng, R. Y. Yang, and H. W. Wu, "Design of a compact CMOS bandpass filter for passive millimeter-wave imaging system application," *Journal of Electromagnetic Waves and Applications*, Vol. 23, Nos. 17–18, 2323–2330, 2009.
2. Yang, X.-D., Y.-S. Li, and C.-Y. Liu, "A toothbrush-shaped patch antenna for millimeter-wave communication," *Journal of Electromagnetic Waves and Applications*, Vol. 23, No. 1, 31–37, 2009.
3. Gu, J., Y. Fan, Y.-H. Zhang, and D.-K. Wu, "A novel 3-D half-mode SICC resonator for microwave and millimeter-wave applications," *Journal of Electromagnetic Waves and Applications*, Vol. 23, Nos. 11–12, 1429–1439, 2009.
4. Shireen, R., S. Shi, and D.-W. Prather, "Wideband millimeter-wave bow-tie antenna," *Journal of Electromagnetic Waves and Applications*, Vol. 23, Nos. 5–6, 737–746, 2009.
5. Oka, S., H. Togo, N. Kukutsu, and T. Nagatsuma, "Latest trends in millimeter-wave imaging technology," *Progress In Electromagnetics Research Letters*, Vol. 1, 197–204, 2008.
6. Kukutsu, N. and Y. Kado, "Overview of millimeter and terahertz wave application research," *NTT Technical Review — Special Feature: Applied Technology for Millimeter and Terahertz Electromagnetic Waves*, Vol. 7, No. 3, 2009.
7. "Millimeter waves: Emerging markets," *Thintry Market Study*, 2012.
8. Liu, J., L. Zhang, S.-H. Fan, C. Guo, S. He, and G.-K. Chang, "A novel architecture for peer-to-peer interconnect in millimeter-wave radio-over-fiber access networks," *Progress In Electromagnetics Research*, Vol. 126, 139–148, 2012.
9. Zhu, B., J. Stiens, V. Matvejev, and R. Vounckx, "Inexpensive and easy fabrication of multi-mode tapered dielectric circular probes

at millimeter wave frequencies," *Progress In Electromagnetics Research*, Vol. 126, 237–254, 2012.

10. Demirci, S., H. Cetinkaya, E. Yigit, C. Ozdemir, and A. A. Vertiy, "A study on millimeter-wave imaging of concealed objects: Application using back-projection algorithm," *Progress In Electromagnetics Research*, Vol. 128, 457–477, 2012.
11. Tahim, R.-S., T. Pham, and K. Chang, "Millimeter-wave microstrip subharmonically pumped mixer," *IEEE Electronics Letters*, Vol. 21, No. 19, 861–862, Sep. 1985
12. Zhao, M., X. Zu, and J. Huang, "Low cost microstrip subharmonic mixer in millimeter wave band," *International Conference on Microwave and Millimeter Wave Technology, ICMMT*, 1–3, Builin, Apr. 18–21, 2007.
13. Guo, J., Z. Xu, C. Qian, and W. Dou, "Design of a microstrip balanced mixer for satellite communication," *Progress In Electromagnetics Research Letters*, Vol. 115, 289–301, 2011.
14. Lin, C.-M., J.-T. Chang, C.-C. Su, S.-H. Hung, and Y.-H. Wang, "A 16–31 GHz miniature quadruple sungarmonic monolithic mixer with lumped diplexer," *Progress In Electromagnetics Research Letters*, Vol. 11, 21–30, 2009.
15. Lin, C.-M., Y.-C. Lee, S.-H. Hung, and Y.-H. Wang, "A 28–40 GHz doubly balanced monolithic passive mixer with a compact IF extraction," *Progress In Electromagnetics Research Letters*, Vol. 19, 171–178, 2010.
16. Lee, Y.-C., C.-M. Lin, S.-H. Hung, C.-C. Su, and Y.-H. Wang, "A broadband doubly balanced monolithic ring mixer with a compact intermediate frequency (IF) extraction," *Progress In Electromagnetics Research Letters*, Vol. 20, 175–184, 2011.
17. Lee, Y.-C., Y.-H. Chang, S. H. Hung, W.-C. Chien, C.-C. Su, C.-C. Hung, C.-M. Lin, and Y.-H. Wang, "A single-balanced quadruple subharmonical mixer with a compact IF extraction," *Progress In Electromagnetics Research Letters*, Vol. 24, 159–167, 2011.
18. Johansen T.-K. and V. Krozer, "A 38 to 44 GHz sub-harmonic balanced HBT mixer with integrated miniature spiral type Marchand balun," *Progress In Electromagnetics Research*, Vol. 135, 317–330, 2013.
19. Lai, Y.-A., S.-H. Hung, C.-N. Chen, and Y.-H. Wang, "A miniature millimeter-wave monolithic star mixer with simple IF extraction circuit," *Journal of Electromagnetic Waves and Applications*, Vol. 23, 2433–2440, 2009.

20. Guo, B. and G. Wen, "Periodic time-varying noise in current-commutating CMOS mixers," *Progress In Electromagnetics Research*, Vol. 117, 283–298, 2011.
21. Lee, S.-J., T.-J. Baek, M. Han, S.-G. Choi, D.-S. Ko, and J.-K. Rhee, "94 GHz MMIC single balanced mixer for FMCW radar sensor application," *5th Global Symposium on Millimeter Waves*, 351–354, Harbin, China, May 27–30, 2012.
22. Fernandez-Garcia, M., S. Ver-Hoeye, C. Vazquez-Antuna, G. R. Hotopan, R. Camblor-Diaz, and F. Las Heras Andres, "Non linear optimization technique for the reduction of the frequency scanning effect in a phased array based on broadband injection-locked third harmonic self-oscillating mixers," *Progress In Electromagnetics Research*, Vol. 127, 479–499, 2012.
23. Fernandez-Garcia, M., S. Ver-Hoeye, C. Vazquez-Antuna, G. R. Hotopan, R. Camblor-Diaz, and F. Las Heras Andres, "New non-linear approach for the evaluation of the linearity of high gain harmonic self oscillating mixers," *Progress In Electromagnetics Research*, Vol. 126, 149–168, 2012.
24. Wan, Q. and C. Wang, "A wideband CMOS current-mode down-conversion mixer for multi-standard receivers," *Progress In Electromagnetics Research*, Vol. 129, 421–437, 2012.
25. Hung, S.-H., W.-C. Chien, C.-M. Lin, Y.-A. Lai, and Y.-H. Wang, "V-band high isolation sub-harmonic monolithic mixer with Hairpin diplexer," *Progress In Electromagnetics Research Letters*, Vol. 16, 161–169, 2010.
26. Zhang, B., Y. Fan, Z. Chen, X. F. Yang, and F. Q. Zhong, "An improved 110–130-GHZ fix-tuned subharmonic mixer with compact microstrip resonant cell structure," *Journal of Electromagnetic Waves and Applications*, Vol. 25, Nos. 2–3, 411–420, Feb. 2011.
27. Ding, D., J. Xu, and Z. Chen, "A W-band low conversion loss single balanced mixer with planar GAAS schottky diodes," *International Conference on Microwave and Millimeter Wave Technology (ICMMT)*, 1–4, Shenzhen, China, May 5–8, 2012.
28. Zhan, M. Z., W. Zhao, and R.-M. Xu, "Design of millimeter-wave wideband mixer with a novel IF block," *Progress In Electromagnetics Research C*, Vol. 30, 41–52, 2012.
29. Morozov, S.-V., K.-S. Novoselov, M.-I. Katsnelson, F. Schedin, D.-C. Elias, J.-A. Jaszczak, and A.-K. Geim, "Giant intrinsic carrier mobilities in graphene and its bilayer," *Physical Review Letters*, Vol. 100, Jan. 2008.
30. Mikhailov, S.-A. and K. Ziegler, "Nonlinear electromagnetic response of graphene: Frequency multiplication and the self-

consistent-field effects," *Journal of Physics: Condensed Matter*, Vol. 20, 384204, 2008.

31. Mikhailov, S.-A., "Electromagnetic response of electrons in graphene: Non-linear effects," *Physica*, Vol. 40, 2626–2629, 2008.
32. Hotopan, G. R., S. Ver-Hoeye, C. Vazquez-Antuna, R. Camblor-Diaz, M. G. Fernandez, F. Las Heras Andres, P. Alvarez, and R. Menndez, "Millimeter wave microstrip mixer based on graphene," *Progress In Electromagnetics Research*, Vol. 118, 57–69, 2011.
33. Ver Hoeye, S., C. Vazquez, M. Gonzalez, M. Fernandez, L. F. Herran, and F. Las Heras, "Multi-harmonic DC-bias network based on arbitrarily width modulated microstrip line," *Progress In Electromagnetics Research Letters*, Vol. 11, 119–128, 2009.
34. Habibpour, O., J. Vukusic, and J. Stake, "A 30-GHz integrated subharmonic mixer based on a multichannel graphene FET," *IEEE Transactions on Microwave Theory and Techniques*, Vol. 61, No. 2, 841–847, 2013.
35. Andersson, M. A., O. Habibpour, J. Vukusic, and J. Stake, "Resistive graphene FET subharmonic mixers: Noise and linearity assessment," *IEEE Transactions on Microwave Theory and Techniques*, Vol. 60, No. 12, 4035–4042, 2012.
36. Lin, Y., A. Garcia, J. Han, D. Farmer, I. Meric, Y. Sun, Y. Wu, C. Dimitrakopoulos, A. Grill, O. Avouris, and K. Jenkins, "Wafer-scale graphene integrated circuit," *Science*, Vol. 332, No. 6035, 1294–1297, 2011.